Geophysical Prospecting, 2008, **56**, 287–292 doi:10.1111/j.1365-2478.2008.00701.x

Seismic reflection coefficients of faults at low frequencies: a model study

Joost van der Neut[1*], Mrinal K. Sen[2] and Kees Wapenaar[1]

[1]*Department of Geotechnology, Delft University of Technology, PO Box 5048, 2600 GA Delft, The Netherlands, and* [2]*University of Texas Institute for Geophysics, John A. and Katherine G. Jackson School of Geosciences, 10100 Burnet Road, Bldg. 196, Austin TX 78758, USA*

Received February 2007, revision accepted February 2008

ABSTRACT

We use linear slip theory to evaluate seismic reflections at non-welded interfaces, such as faults or fractures, sandwiched between general anisotropic media and show that at low frequencies the real parts of the reflection coefficients can be approximated by the responses of equivalent welded interfaces, whereas the imaginary parts can be related directly to the interface compliances. The imaginary parts of low frequency seismic reflection coefficients at fault zones can be used to estimate the interface compliances, which can be related to fault properties upon using a fault model. At normal incidence the expressions uncouple and the complex-valued P-wave reflection coefficient can be related linearly to the normal compliance. As the normal compliance is highly sensitive to the infill of the interface, it can be used for gas/fluid identification in the fault plane. Alternatively, the tangential compliance of a fault can be estimated from the complex-valued S-wave reflection coefficient. The tangential compliance can provide information on the crack density in a fault zone. Coupling compliances can be identified and quantified by the observation of PS conversion at normal incidence, with a comparable linear relationship.

INTRODUCTION

Faults or fractures can cause a discontinuity in the particle velocity of an elastic wavefield. In linear slip theory, we assume that the particle velocity discontinuity can be related linearly to the interface traction through the normal and tangential interface compliances, assuming continuity of traction (Schoenberg 1980; Kitsunezaki 1983; Gu *et al.* 1996; Groenenboom and Fokkema 1998). Seismic reflection coefficients at a single non-welded interface have been studied by various authors analytically, numerically and in laboratory experiments (Pyrak-Nolte, Myer and Cook 1990; Haugen and Schoenberg 2000; Chaisri and Krebes 2000). Nakagawa, Nihei and Myer (2000) showed that fractures under shear stress may give wave conversion at normal incidence, which can be explained by extending the linear slip model with coupling compliances. Other authors have modelled the particle velocity discontinuity by interpreting the fault as a planar distribution of cracks on a welded surface (Hudson, Liu and Crampin 1996) or as a planar distribution of welded contact areas on a free surface (Hudson, Liu and Crampin 1997). Reflection and transmission coefficients at non-welded interfaces are complex-valued, yielding distortions of both amplitude and phase of a reflecting or transmitting wavefield. Pyrak-Nolte *et al.* (1990) give various references to laboratory and field observations supporting linear slip theory.

In this paper we take Haugen and Schoenberg (2000) as a starting point by modelling seismic reflection coefficients at a non-welded interface between two general anisotropic layers. We show that at low frequencies the real parts of the reflection coefficients approximate the coefficients of an equivalent welded interface and the imaginary parts can be related directly to the interface compliances. In an isotropic

* E-mail: j.r.vanderneut@tudelft.nl

background, fault models by Hudson and Liu (1999) can be used to relate the tangential interface compliance to physical fault properties. The ratio of normal and tangential compliances can be used as a fluid indicator, as suggested by Schoenberg and Sayers (1995).

REFLECTION MODEL

We start with a brief review of linear slip theory and the derivation of seismic reflection coefficients at a non-welded interface between two general anisotropic layers. Consider a horizontal non-welded interface in 3-dimensional space. We apply Fourier transformation of the wavefields with respect to time (t) and lateral coordinates (x_1, x_2, x_3), using the definition: $\tilde{f}(k_1, k_2, x_3, \omega) = \int_{-\infty}^{+\infty}\int_{-\infty}^{+\infty}\int_{-\infty}^{+\infty} f(x_1, x_2, x_3, t)\exp(-i\omega t + ik_1x_1 + ik_2x_2)dtdx_1 dx_2$, with i denoting the imaginary unit, k_1 and k_2 being horizontal wavenumbers and ω the angular frequency. We assume that the traction vector $\tilde{\boldsymbol{\tau}}_3$ is continuous at the interface, whereas the particle velocity vector $\tilde{\mathbf{v}}$ is not. We introduce the jump of particle velocity as $[\tilde{\mathbf{v}}] = \tilde{\mathbf{v}}_{II} - \tilde{\mathbf{v}}_I$. Subscripts I and II refer to the media at the upper and lower side of the interface, respectively, throughout this paper. The discontinuity of particle velocity can be related to the interface traction through the interface compliance matrix $\mathbf{Z}$ (Schoenberg 1980):

$$[\tilde{\mathbf{v}}] = i\omega\mathbf{Z}\tilde{\boldsymbol{\tau}}_3. \tag{1}$$

Here, $\mathbf{Z}$ is assumed to have the following structure:

$$\mathbf{Z} = \begin{pmatrix} Z_T & Z_{12} & Z_{13} \\ Z_{12} & Z_T & Z_{23} \\ Z_{13} & Z_{23} & Z_N \end{pmatrix}, \tag{2}$$

where Z_N is the normal compliance, Z_T is the tangential compliance and Z_{12}, Z_{13} and Z_{23} are coupling compliances. All interface compliances are assumed real-valued, implying that no energy is dissipated at the interface. Equation (1) can also be evaluated in a 2D configuration, by writing the compliance matrix as

$$\mathbf{Z} = \begin{pmatrix} Z_T & Z_C \\ Z_C & Z_N \end{pmatrix}, \tag{3}$$

where Z_C is the coupling compliance. The assumption of continuous traction can be combined with equation (1), yielding the following boundary condition for the non-welded interface:

$$\begin{pmatrix} \tilde{\mathbf{v}}_{II} \\ \tilde{\boldsymbol{\tau}}_{3,II} \end{pmatrix} = \begin{pmatrix} \mathbf{I} & i\omega\mathbf{Z} \\ \mathbf{O} & \mathbf{I} \end{pmatrix} \begin{pmatrix} \tilde{\mathbf{v}}_{I} \\ \tilde{\boldsymbol{\tau}}_{3,I} \end{pmatrix}, \tag{4}$$

where $\mathbf{I}$ is the identity matrix and $\mathbf{O}$ is the null matrix. Particle velocity $\tilde{\mathbf{v}}$ and traction $\tilde{\boldsymbol{\tau}}_3$ can be decomposed into the wave vectors of the downgoing and upgoing wavefields $\tilde{\mathbf{w}}^+$ and $\tilde{\mathbf{w}}^-$, respectively (Woodhouse 1974; Ursin 1983; Wapenaar and Berkhout 1989). We scale the decomposition such that the components of $\tilde{\mathbf{w}}^\pm$ represent the particle velocities of the individual wave modes; that is: $\tilde{\mathbf{w}}^\pm = (\,\tilde{v}^{P,\pm}\ \tilde{v}^{Sh,\pm}\ \tilde{v}^{Sv,\pm}\,)^T$. Here $\tilde{v}^{X,\pm}$ is the complex amplitude of the particle velocity of the down- or upgoing quasi-X-mode wavefield and superscript T denotes transposition. The wave vectors are related to the particle velocity and traction through

$$\begin{pmatrix} \tilde{\mathbf{v}} \\ \tilde{\boldsymbol{\tau}}_3 \end{pmatrix} = \begin{pmatrix} \tilde{\mathbf{L}}_1^+ & \tilde{\mathbf{L}}_1^- \\ \tilde{\mathbf{L}}_2^+ & \tilde{\mathbf{L}}_2^- \end{pmatrix} \begin{pmatrix} \tilde{\mathbf{w}}^+ \\ \tilde{\mathbf{w}}^- \end{pmatrix}, \tag{5}$$

where $\tilde{\mathbf{L}}_1^\pm$ and $\tilde{\mathbf{L}}_2^\pm$ are composition matrices, derived by eigenvalue decomposition of matrix $\mathbf{A}$ of Woodhouse (1974). We perform the decomposition at the upper and lower side of the interface and substitute the results into equation (4), yielding

$$\begin{pmatrix} \tilde{\mathbf{L}}_{1,II}^+ & \tilde{\mathbf{L}}_{1,II}^- \\ \tilde{\mathbf{L}}_{2,II}^+ & \tilde{\mathbf{L}}_{2,II}^- \end{pmatrix} \begin{pmatrix} \tilde{\mathbf{w}}_{II}^+ \\ \tilde{\mathbf{w}}_{II}^- \end{pmatrix} = \begin{pmatrix} \mathbf{I} & i\omega\mathbf{Z} \\ \mathbf{O} & \mathbf{I} \end{pmatrix} \begin{pmatrix} \tilde{\mathbf{L}}_{1,I}^+ & \tilde{\mathbf{L}}_{1,I}^- \\ \tilde{\mathbf{L}}_{2,I}^+ & \tilde{\mathbf{L}}_{2,I}^- \end{pmatrix} \begin{pmatrix} \tilde{\mathbf{w}}_{I}^+ \\ \tilde{\mathbf{w}}_{I}^- \end{pmatrix}. \tag{6}$$

Consider an incident downgoing wavefield in the upper medium $\tilde{\mathbf{w}}_I^+$, reflecting at the interface, with the upgoing wavefield in the lower medium $\tilde{\mathbf{w}}_{II}^-$ being absent. We introduce reflection coefficient matrix $\tilde{\mathbf{R}}$ to describe the upgoing wavefield in the upper medium as $\tilde{\mathbf{w}}_I^- = \tilde{\mathbf{R}}\tilde{\mathbf{w}}_I^+$. As the components of the wave vectors correspond to the individual wave modes, $\tilde{\mathbf{R}}$ has the following structure:

$$\tilde{\mathbf{R}} = \begin{pmatrix} \tilde{R}^{PP} & \tilde{R}^{PSh} & \tilde{R}^{PSv} \\ \tilde{R}^{ShP} & \tilde{R}^{ShSh} & \tilde{R}^{ShSv} \\ \tilde{R}^{SvP} & \tilde{R}^{SvSh} & \tilde{R}^{SvSv} \end{pmatrix}, \tag{7}$$

where $\tilde{R}^{XY}$ represents the reflection coefficient relating the reflected quasi-X-mode to the incident quasi-Y-mode. Similarly, a 3×3 transmission matrix $\tilde{\mathbf{T}}$ is introduced via $\tilde{\mathbf{w}}_{II}^+ = \tilde{\mathbf{T}}\tilde{\mathbf{w}}_I^+$. Substituting these formulations into boundary condition (6) yields

$$\begin{pmatrix} \tilde{\mathbf{L}}_{1,II}^+ & \tilde{\mathbf{L}}_{1,II}^- \\ \tilde{\mathbf{L}}_{2,II}^+ & \tilde{\mathbf{L}}_{2,II}^- \end{pmatrix} \begin{pmatrix} \tilde{\mathbf{T}} \\ \mathbf{O} \end{pmatrix} = \begin{pmatrix} \mathbf{I} & i\omega\tilde{\mathbf{Z}} \\ \mathbf{O} & \mathbf{I} \end{pmatrix} \begin{pmatrix} \tilde{\mathbf{L}}_{1,I}^+ & \tilde{\mathbf{L}}_{1,I}^- \\ \tilde{\mathbf{L}}_{2,I}^+ & \tilde{\mathbf{L}}_{2,I}^- \end{pmatrix} \begin{pmatrix} \mathbf{I} \\ \tilde{\mathbf{R}} \end{pmatrix}. \tag{8}$$

We can solve equation (8) for $\tilde{\mathbf{R}}$ as

$$\tilde{\mathbf{R}} = -\left(\tilde{\Xi}^{-} - i\omega\mathbf{Z}\tilde{\mathbf{L}}^{-}_{2,I}\right)^{-1}\left(\tilde{\Xi}^{+} - i\omega\mathbf{Z}\tilde{\mathbf{L}}^{+}_{2,I}\right), \tag{9}$$

with

$$\tilde{\Xi}^{\pm} = \tilde{\mathbf{L}}^{+}_{1,II}\left(\tilde{\mathbf{L}}^{+}_{2,II}\right)^{-1}\tilde{\mathbf{L}}^{\pm}_{2,I} - \tilde{\mathbf{L}}^{\pm}_{1,I}. \tag{10}$$

Equation (9) allows us to compute exact reflection coefficients of all (quasi) wave modes and their conversions at a non-welded interface between general anisotropic media and is similar to equation (A10) of Haugen and Schoenberg (2000).

LOW FREQUENCY APPROXIMATION

Our purpose is to evaluate the precritical seismic reflection coefficient matrix at low frequencies. As in this regime the elements of $\omega\mathbf{Z}\tilde{\mathbf{L}}^{-}_{2,I}$ are small compared to their counterparts of $\tilde{\Xi}^{-}$, equation (9) can be split in a real part that resembles the reflection matrix of an equivalent welded interface, $\tilde{\mathbf{R}}_0 = -(\tilde{\Xi}^{-})^{-1}\tilde{\Xi}^{+}$, and an imaginary part as induced by the slip:

$$\tilde{\mathbf{R}} \approx \tilde{\mathbf{R}}_0 + i\tilde{\mathbf{R}}_{SLIP}, \tag{11}$$

with

$$\tilde{\mathbf{R}}_{SLIP} = \omega\left(\tilde{\Xi}^{-}\right)^{-1}\mathbf{Z}\left(\tilde{\mathbf{L}}^{+}_{2,I} + \tilde{\mathbf{L}}^{-}_{2,I}\tilde{\mathbf{R}}_0\right). \tag{12}$$

The imaginary part of the reflection matrix $\tilde{\mathbf{R}}_{SLIP}$ can thus be used directly as an indicator for the interface compliance matrix $\mathbf{Z}$. When evaluated in isotropic media, equation (12) uncouples for the special case of normal incidence and we find four expressions relating each single component of the reflection coefficient matrix to a single component of the interface compliance. We find for the diagonal terms:

$$\Im\{A^{PP}\} \approx -\left(\frac{1}{\rho_I\alpha_I} + \frac{1}{\rho_{II}\alpha_{II}}\right)^{-1}\left(1 + A_0^{PP}\right)\omega Z_N, \tag{13}$$

$$\Im\{A^{SS}\} \approx -\left(\frac{1}{\rho_I\beta_I} + \frac{1}{\rho_{II}\beta_{II}}\right)^{-1}\left(1 + A_0^{SS}\right)\omega Z_T. \tag{14}$$

Here, $\Im\{A^{PP}\}$ and $\Im\{A^{SS}\}$ stand for the imaginary parts of the PP and SS reflection intercepts (= the reflection coefficients at normal incidence), α, β and ρ are the P-wave velocity, S-wave velocity and density of the media that subscripts I and II refer to and A_0^{PP} and A_0^{SS} are the PP and SS reflection intercepts of the equivalent welded interface. Equations (13) and (14) allow us to estimate the normal and tangential interface compliances directly from the imaginary parts of the intercepts of P- and S-wave reflections. In the appendix we show how the tangential compliance can be related to physical properties of a fault, using models by Hudson and Liu (1999). The ratio of normal and tangential compliance can be used as a fluid indicator, providing insight in the fault infill conditions (Schoenberg and Sayers 1995; Lubbe *et al.* 2007). For fluid saturation we find that $Z_N^{FLUID} = 0$, whereas for gas saturation $Z_N^{GAS} = (1 - \frac{\bar{\nu}}{2})Z_T$ (Hudson 1981), where $\bar{\nu}$ is the Poisson's ratio of the average background rock.

When the properties of upper and lower media are the same, that is $\alpha_I = \alpha_{II} = \alpha$, $\beta_I = \beta_{II} = \beta$ and $\rho_I = \rho_{II} = \rho$, equations (13) and (14) simplify to

$$\Im\{A^{PP}\} \approx -\frac{\rho\alpha}{2}\omega Z_N, \tag{15}$$

$$\Im\{A^{SS}\} \approx -\frac{\rho\beta}{2}\omega Z_T. \tag{16}$$

These expressions are equal to the low frequency approximation of equation (21) of Pyrak-Nolte *et al.* (1990) for non-welded interfaces without contrast of medium parameters (note the sign difference, which is related to our definition of the Fourier transform).

Low frequency slip induced PS conversion at normal incidence can be directly quantified from the off-diagonal terms that arise from evaluation of equation (12) in an isotropic background at normal incidence, yielding

$$\Im\left\{A^{SP}\right\} \approx \frac{\alpha_I}{\beta_I}\left(\frac{1}{\rho_I\beta_I} + \frac{1}{\rho_{II}\beta_{II}}\right)^{-1}\left(1 + A_0^{PP}\right)\omega Z_C, \tag{17}$$

$$\Im\left\{A^{PS}\right\} \approx \frac{\beta_I}{\alpha_I}\left(\frac{1}{\rho_I\alpha_I} + \frac{1}{\rho_{II}\alpha_{II}}\right)^{-1}\left(1 + A_0^{SS}\right)\omega Z_C, \tag{18}$$

where $\Im\{A^{SP}\}$ and $\Im\{A^{PS}\}$ stand for the imaginary parts of the P-to-S and S-to-P reflection intercepts, respectively. As an equivalent welded interface will generally have no converted wave in this special case, the real parts of the converted reflection intercepts of the non-welded interface will be close to zero in the low frequency regime (due to equation 11) and the imaginary parts will equal the magnitudes, which can be used as direct indicators for the coupling compliance through equations (17) and (18).

EXAMPLES

In the first example we model seismic P-wave reflection coefficients at a frequency of 30 Hz at four different fault interfaces, with properties as given in Table 1. The faults are at an angle of 60 degrees with respect to the horizontal plane and they are sandwiched between vertical transverse isotropic (VTI) shale and sandstone with properties as given in Table 2. We choose a new coordinate system such that the fault is aligned

with the horizontal plane, implying rotation of the media's stiffnesses over 60 degrees, using Bond transformation matrices (Auld 1973). Figure 1 shows the imaginary parts of the reflection coefficients with varying angles of incidence, evaluated with equation (9) (coloured solid lines) as well as with low frequency approximation (12) (black dashed lines). Note that the effects of slip are best manifested at normal incidence and that the low frequency approximations match closely the exact responses. Next, we evaluate the imaginary parts of the reflection intercepts with varying frequencies, exact (equation 9) and with the low frequency approximation (equation 12) – see Fig. 2. The low frequency approximation matches closely the exact results for all four interfaces for frequencies up to 60 Hz.

In another example we model PS converted reflection coefficients at a frequency of 30 Hz at four fault interfaces with different coupling compliances; their properties being given in Table 3. The faults are sandwiched between isotropic shale with P-wave velocity $\alpha_I = 2730m/s$, S-wave velocity $\beta_I = 1240m/s$ and density $\rho_I = 2350m/s$ and isotropic sandstone with P-wave velocity $\alpha_{II} = 2020m/s$, S-wave velocity $\beta_{II} = 1230m/s$ and density $\rho_{II} = 2130m/s$. Figure 3 shows the imaginary parts of the PS converted reflection coefficients with varying angles of incidence. Note that the low frequency approximations match closely the exact responses for all

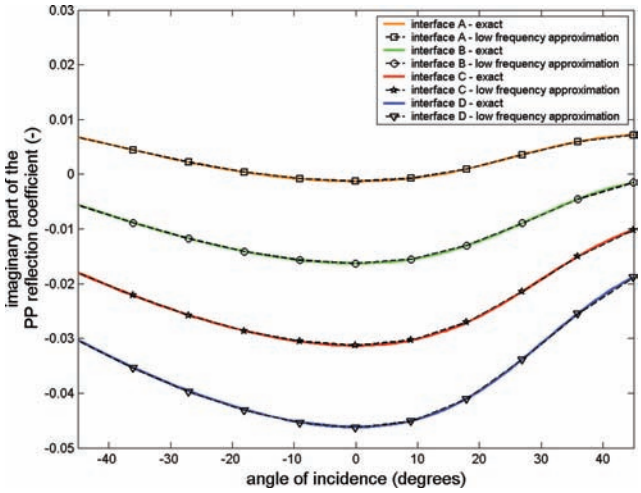

Figure 1 Imaginary parts of the PP reflection coefficients of interfaces A, B, C and D with varying angles of incidence; solid lines are exact; dashed lines are in the low frequency approximation.

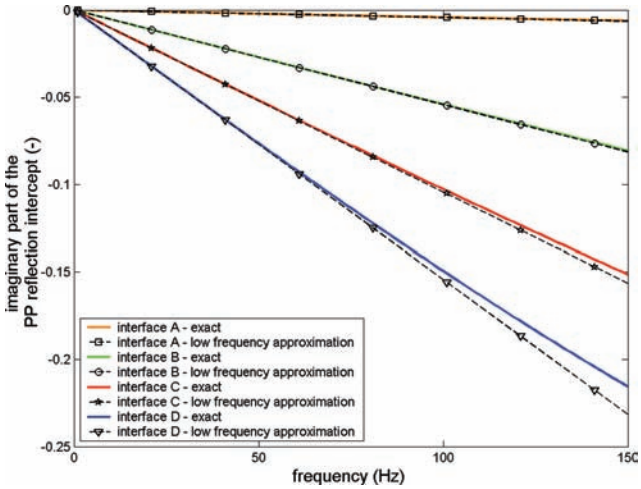

Figure 2 Frequency dependence of the imaginary parts of the PP reflection intercepts of interfaces A, B, C and D; solid lines are exact; dashed lines are in the low frequency approximation.

Table 1 Properties of interfaces A, B, C and D; note that the compliance ratios range from 0 (= fluid saturated) for interface A to $7.0/8.1 \approx 1 - \bar{\nu}/2$ (= gas saturated) for interface DP

Interface	A	B	C	D
normal compliance ($\cdot 10^{-11}\ m/Pa$)	0.0	2.3	4.6	7.0
tangential compliance ($\cdot 10^{-11}\ m/Pa$)	8.1	8.1	8.1	8.1
coupling compliance ($\cdot 10^{-11}\ m/Pa$)	0.0	0.0	0.0	0.0

Table 2 Stiffnesses and densities of a VTI shale (medium I) and a VTI sandstone (medium II); stiffnesses are expressed in the Voigt notation, relating to the $4 \times 4 \times 4 \times 4$ stiffness tensor through the following relations: $c_{1111} = c_{2222} = C_{11}$, $c_{3333} = C_{33}$, $c_{1133} = c_{3311} = c_{2233} = c_{3322} = C_{13}$, $c_{1313} = c_{3131} = c_{2323} = c_{3232} = C_{44}$, $c_{1212} = c_{2121} = C_{66}$, $c_{1122} = c_{2211} = C_{11} - 2C_{66}$ and all other c_{ijkl} being zero; data taken from Wang (2002)

Quantity	C_{11} (GPa)	C_{33} (GPa)	C_{13} (GPa)	C_{44} (GPa)	C_{66} (GPa)	ρ (kg/ m^3)
Shale	43.25	27.58	13.45	6.59	13.31	2511
Sandstone	34.28	34.11	14.62	10.11	9.56	2307

Table 3 Properties of interfaces E, F, G and H

Interface	E	F	G	H
normal compliance ($\cdot 10^{-11}$ m/Pa)	12	12	12	12
tangential compliance ($\cdot 10^{-11}$ m/Pa)	15	15	15	15
coupling compliance ($\cdot 10^{-11}$ m/Pa)	0	4	8	12

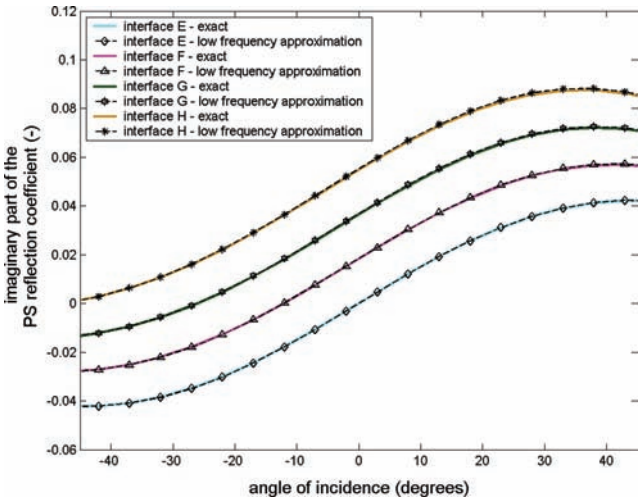

Figure 3 Imaginary parts of the PS reflection coefficients of interfaces E, F, G and H with varying angles of incidence; solid lines are exact; dashed lines are in the low frequency approximation.

interfaces. At normal incidence the real parts vanish and equation (17) can be used for direct quantification of the coupling compliance from the PS converted reflection intercept's magnitude.

CONCLUSION

We have used linear slip theory to derive general expressions for seismic reflection coefficients at non-welded interfaces, such as faults or fractures, between general anisotropic media and approximated these coefficients at low frequencies (<60 Hz). We showed that the real parts of these approximated reflection coefficients match the responses of the equivalent welded interfaces, whereas the slip induced parts are purely imaginary in this regime. The effects of slip could be observed by phase changes in seismic reflection data.

By combination of amplitude and phase information, the real and imaginary parts of reflection coefficients at faults / non-welded interfaces can be extracted. The imaginary parts of these coefficients can be related to the interface compliances of a fault. For the special case of an isotropic background and normal incidence, the system uncouples and we find simple linear expressions, which can be used to estimate the normal compliance directly from complex-valued PP data and the tangential compliance from equivalent SS data. Off-diagonal terms of the interface compliance matrix can yield normal incident P-to-S or S-to-P converted reflections, which can provide additional information on the interface roughness.

REFERENCES

Auld B. A. 1973. *Acoustic Fields and Waves in Solids*. Wiley, New York.

Chaisri S. and Krebes E.S. 2000. Exact and approximate formulas for P-Sv reflection and transmission coefficients for a nonwelded contact interface. *Journal of Geophysical Research* **105**, 28.045–28.054.

Groenenboom J. and Fokkema J.T. 1998. Monitoring the width of hydraulic fractures with acoustic waves. *Geophysics* **63**, 139–148.

Gu B., Suárez-Rivera R., Nihei K.T. and Myer L.R. 1996. Incidence of plane waves upon a fracture. *Journal of Geophysical Research* **101**, 25.337–25.346.

Haugen G.U. and Schoenberg M.A. 2000. The echo of a fault or fracture. *Geophysics* **65**, 176–189.

Hudson J.A. 1981. Wave speeds and attenuation of elastic waves in material containing cracks. *Geophysical Journal of the Royal Astronomical Society* **64**, 133–150.

Hudson J.A. and Liu E. 1999. Effective elastic properties of heavily faulted structures. *Geophysics* **64**, 479–485.

Hudson J.A., Liu E. and Crampin S. 1996. Transmission properties of a plane fault. *Geophysical Journal International* **125**, 559–566.

Hudson J.A., Liu E. and Crampin S. 1997. The mean transmission properties of fault with imperfect facial contact. *Geophysical Journal International* **129**, 720–726.

Kitsunezaki C. 1983. Behavior of plane elastic waves across a plane crack. *Journal of Mining College of Atika University* **6**, 173–187.

Lubbe R., Sothcott J., Worthington M.H. and McCann C. 2007. Laboratory estimates of normal/shear fracture compliance ratio. 69th EAGE meeting, London, UK, Expanded Abstracts, F026.

Nakagawa S., Nihei K.T. and Myer L.R. 2000. Shear-induced conversion of seismic waves across single fractures. *International Journal of Rock Mechanics and Mining Sciences* **37**, 203–218.

Pyrak-Nolte L.J., Myer L.R. and Cook N.G.W. 1990. Transmission of seismic waves across single natural fractures. *Journal of Geophysical Research* **95**, 8617–8638.

Schoenberg M. 1980. Elastic wave behavior across linear slip interfaces. *Journal of the Acoustical Society of America* **68**, 1516–1521.

Schoenberg M. and Sayers C.M. 1995. Seismic anisotropy of fractured rock. *Geophysics* **60**, 204–211.

Ursin B. 1983. Review of elastic and electromagnetic wave propagation in horizontally layered media. *Geophysics* **48**, 1063–1081.

Wang Z. 2002. Seismic anisotropy in sedimentary rocks, part 2: Laboratory data. *Geophysics* **67**, 1423–1440.

Wapenaar C.P.A. and Berkhout A.J. 1989. *Elastic Wave Field Extrapolation, Redatuming of Single and Multi-component Seismic Data*. Elsevier, Amsterdam.

Woodhouse J.H. 1974. Surface waves in a laterally varying layered structure. *Geophysical Journal of the Royal Astronomical Society* **37**, 461–490.

APPENDIX: FAULT MODELS

To interpret the tangential interface compliance in an isotropic medium, we can make use of fault models. Here, we use a model by Hudson and Liu (1999), representing a non-welded interface or fault as a planar distribution of cracks with average crack size a and planar crack density e^S. The cracks are evaluated in an average background medium, described by density $\bar{\rho} = (\rho_I + \rho_{II})/2$, P-wave velocity $\bar{\alpha} = (\alpha_I + \alpha_{II})/2$ and S-wave velocity $\bar{\beta} = (\beta_I + \beta_{II})/2$. The tangential compliance can be formulated as

$$Z_T = \frac{16\bar{\alpha}^2}{3\bar{\rho}\bar{\beta}^2\left(3\bar{\alpha}^2 - 2\bar{\beta}^2\right)}\left(1 + \frac{4\pi}{3}\left(e^S\right)^{\frac{2}{3}}\right)e^S a. \tag{A1}$$

Heavily fractured faults can be interpreted as a planar distribution of welded contact areas on a free surface. If e^S_W is the planar density of the contact areas and b the average size of these areas, the tangential compliance can be computed as

$$Z_T = \frac{3\bar{\alpha}^2 - 2\bar{\beta}^2}{8\bar{\rho}\bar{\beta}^2\left(\bar{\alpha}^2 - \bar{\beta}^2\right)}\left(1 + 2\left(e^S_W\right)^{\frac{1}{2}}\right)^{-1}\frac{b}{e^S_W}. \tag{A2}$$

Expressions (A1) and (A2) can form a basis for physical interpretation of the estimated tangential compliance of a fault. They can be averaged over different fault planes to represent a fault zone (Hudson and Liu 1999).